第 36 卷第 6 期
2020 年 6 月

无 机 化 学 学 报
CHINESE JOURNAL OF INORGANIC CHEMISTRY

Vol.36 No.6
1185-1194

锰有机膦酸配位聚合物的合成、结构和磁性

刘 蓓 鲍松松 任 旻 蔡中胜 刘景翠 郑丽敏*
(南京大学化学化工学院,配位化学国家重点实验,南京 210023)

摘要：将 4-羧酸-1-萘膦酸(4-cnappH_3)与氯化锰通过水热(溶剂热)反应,得到 4 种不同结构的锰萘膦酸羧酸配位聚合物 Mn(4-cnappH_2)$_2$ (**1**),Mn(4-cnappH_2)$_2$(H_2O)$_2$ (**2**),α-Mn(4-cnappH)(H_2O) (**3**)和β-Mn(4-cnappH)(H_2O) (**4**)。化合物 **1** 中{MnO_6}八面体与{PO_3C}四面体共角连接形成无机链,链与链之间通过膦酸配体连接形成三维框架结构,而化合物 **2**~**4** 都具有层状结构,层与层之间由质子化的羧酸基团通过氢键作用连接形成三维超分子结构。但这些化合物的层内拓扑结构不同,化合物 **2** 中的无机层结构包含由{MnO_6}八面体和{PO_3C}四面体共角连接的矩形 12 元环,化合物 **3** 中{MnO_5}三角双锥共边形成{Mn_2O_2}双核,双核之间通过{PO_3C}四面体共角连接形成包含 4 元环的无机层,而化合物 **4** 中则存在由{MnO_5}三角双锥共角形成的链,链间进一步通过{PO_3C}四面体共角连接形成包含 3 元环和 4 元环的无机层。磁性研究表明,所有化合物中锰离子之间都存在反铁磁相互作用。

关键词：有机膦酸；锰配合物；配位聚合物；层状；磁性
中图分类号：O614.71$^+$1　　**文献标识码**：A　　**文章编号**：1001-4861(2020)06-1185-10
DOI：10.11862/CJIC.2020.132

Syntheses, Structures and Magnetic Properties of Manganese Phosphonates

LIU Bei　BAO Song-Song　REN Min　CAI Zhong-Sheng　LIU Jing-Cui　ZHENG Li-Min*
(*State Key Laboratory of Coordination Chemistry, School of Chemistry and Chemical Engineering, Nanjing University, Nanjing* 210023, *China*)

Abstract: Reactions of (4-carboxynaphthalen-1-yl)phosphonic acid (4-cnappH_3) with manganese chloride under solvo/hydrothermal conditions resulted in four new coordination polymers, formulated as Mn(4-cnappH_2)$_2$ (**1**), Mn(4-cnappH_2)$_2$(H_2O)$_2$ (**2**), α-Mn(4-cnappH)(H_2O) (**3**) and β-Mn(4-cnappH)(H_2O) (**4**). Compound **1** shows a 3D framework structure, where chains made up of corner-sharing {MnO_6} octahedra and {PO_3C} tetrahedra are cross-linked by the organic groups of the phosphonate ligands. Compounds **2**~**4** exhibit 2D layered structures with interlayer hydrogen bonds through the pendent carboxylic acid groups. However, the layer topologies are different in the three cases. In **2**, the {MnO_6} octahedra and {PO_3C} tetrahedra are corner-shared with each other alternatively, forming an inorganic layer containing rectangular-shaped 12-membered rings. In **3**, edge-sharing dimers of {Mn_2O_2} are connected by {PO_3C} tetrahedra through corner-sharing, forming an inorganic layer containing 4-membered rings. In **4**, chains of corner-sharing {MnO_5} are connected by {PO_3C} tetrahedra into an inorganic layer containing 3- and 4-membered rings. Magnetic studies reveal that antiferromagnetic interactions are dominant in all four compounds. CCDC: 1990441, **1**; 1990442, **2**; 1990443, **3**; 1990444, **4**.

Keywords: phosphonate; manganese; coordination polymer; magnetic

收稿日期:2020-03-27。收修改稿日期:2020-04-16。
国家自然科学基金(No.21731003)资助项目。
*通信联系人。E-mail:lmzheng@nju.edu.cn

Metal-organic systems have provided tremendous possibilities in building up new molecular materials with potential applications in various areas such as sorption and separation, catalysis, sensors and other functional materials[1-3]. As an important class of metal-organic materials, metal phosphonates possess advantages over many others in their high water and thermal stabilities due to the strong coordination capabilities of the phosphonate ligands and the presence of inorganic components (cluster, chains and layers) in the molecular composite[4]. During the past two decades, great efforts have been devoted to the syntheses of metal phosphonates with new architectures and interesting physical or chemical functions[5-8]. Among them, metal phosphonates containing carboxylate groups are of particular interest as they provide additional coordination sites for metal ions[4]. For example, by using 2/3/4-carboxyphenylphosphonic acid (2/3/4-cppH$_3$) as reaction precursor, a series of metal phosphonate compounds with 1D, 2D and 3D structures have been reported[9], and some of them show interesting magnetic[10], dielectric[11] and chiroptical properties[12]. The (4-carboxynaphthalen-1-yl)phosphonic acid (4-cnappH$_3$) is analogues to 4-cppH$_3$ except with an expanded aromatic moiety. However, only four metal phosphonates based on this ligand have been described, including a cobalt compound with 3D framework structure showing enantioenrichment[13] and three copper compounds with layered structures[14]. To explore new aromatic phosphonate-carboxylate materials, herein we report four new manganese phosphonates based on 4-cnappH$_3$, formulated as Mn(4-cnappH$_2$)$_2$ (**1**), Mn(4-cnappH$_2$)$_2$(H$_2$O)$_2$ (**2**), α-Mn(4-cnappH)(H$_2$O) (**3**) and β-Mn(4-cnappH)(H$_2$O) (**4**). Compound **1** shows a 3D framework structure, whereas **2**~**4** exhibit 2D layered structures but with different layer topologies. The magnetic properties of all four compounds are also investigated.

1 Experimental

1.1 Materials and characterization

The (4-carboxynaphthalen-1-yl)phosphonic acid (4-cnappH$_3$) was synthesized according to the literature method[13,15]. All the other starting materials were obtained from commercial sources without further purification. Elemental analysis for C, H, N were performed on a Perkin-Elmer 240C elemental analyzer. The infrared spectra were recorded on a Bruker Tensor 27 spectrometer with pressed KBr pellets in the 400~4 000 cm^{-1} region. Powder X-ray diffraction patterns (PXRD) were recorded in 2θ range of 3°~50° on a Bruker D8 ADVANCE X-ray powder diffractometer (40 kV and 40 mA) using Cu $K\alpha$ radiation (λ= 0.154 18 nm) at room temperature. The magnetic susceptibility data were obtained using polycrystalline samples by a Quantum Design MPMS-XL7 SQUID magnetometer or MPMS SQUID VSM. The diamagnetic contribution of the sample itself was estimated from Pascal′s constant[16].

1.2 Syntheses of manganese phosphonates

1.2.1 Synthesis of Mn(4-cnappH$_2$)$_2$ (**1**)

A mixture of MnCl$_2$·4H$_2$O (0.029 9 g, 0.15 mmol) and 4-cnappH$_3$ (0.025 3 g, 0.10 mmol) in 10 mL of H$_2$O/methanol (2∶3, *V*/*V*), adjusted to pH=3.05 with 0.5 mol·L^{-1} NaOH and 0.5 mol·L^{-1} HCl, was kept in a Teflon-lined autoclave at 100 ℃ for 3 d. After cooling to room temperature, light yellow block-like polycrystalline materials of **1** were obtained as a pure phase, confirmed by the powder XRD measurements (Fig.S1). Yield: 40.8% (based on 4-cnappH$_3$). Elemental analysis found (Calcd.) for C$_{22}$H$_{16}$O$_{10}$P$_2$Mn(%): C, 48.01(47.41); H, 3.01(2.90). IR (KBr, cm^{-1}): 3 425(b,m), 2 902(b,m), 1 678(s), 1 584(w), 1 513(m), 1 463(w), 1 421(m), 1 319(m), 1 302(w), 1 211(m), 1 153(m), 1 106(vs), 1 078(m), 1 044(vs), 1 015(vs), 961(s), 903(m), 858(m), 788(m), 741(m), 674(m), 624(m).

1.2.2 Synthesis of Mn(4-cnappH$_2$)$_2$(H$_2$O)$_2$ (**2**)

Compound **2** was synthesized following a similar procedure to compound **1** except that the pH value of the reaction mixture was 3.80. Colorless plate-like crystals were obtained as a pure phase, confirmed by the powder XRD measurements (Fig.S1). Yield: 34.4% (based on 4-cnappH$_3$). Elemental analysis found (Calcd.) for C$_{22}$H$_{20}$O$_{12}$P$_2$Mn$_2$(%): C, 44.95(44.54); H, 3.43(3.40). IR (KBr, cm^{-1}): 3 628(m), 3 576(m), 3 414(m), 3 088(b,m), 1 709(s), 1 652(m), 1 633(m), 1 578

(w), 1 515(m), 1 459(m), 1 404(w), 1 279(m), 1 249 (m), 1 187(s), 1 167(m), 1 121(s), 1 048(vs), 1 007(m), 944(m), 904(m), 858(w), 797(w), 774(s), 675(m).

1.2.3　Synthesis of α-Mn(4-cnappH)(H_2O) (**3**)

Compound **3** was synthesized following a similar procedure to compound **1** except that the solvent was pure water (6 mL) and the pH value of the reaction mixture was 3.60. Colorless plate-like crystals were obtained as a pure phase, confirmed by the powder XRD measurements (Fig.S1). Yield: 34.4% (based on 4-cnappH_3). Elemental analysis found (Calcd.) for $C_{11}H_9O_6PMn$(%): C, 40.56(40.89); H, 3.01(2.79). IR (KBr, cm^{-1}): 3 332(b,m), 3 055(b,m), 2 361(w), 1 694 (s), 1 580(m), 1 515(m), 1 458(w), 1 353(w), 1 309(m), 1 284(m), 1 257(m), 1 203(m), 1 153(w), 1 126(m), 1 081(vs), 1 034(vs), 1 017(vs), 984(s), 927(m), 855 (w), 794(w), 773(s), 677(m), 614 (m).

1.2.4　Synthesis of β-Mn(4-cnappH)(H_2O) (**4**)

Compound **4** was synthesized following a similar procedure to **3** except that the pH value of the reaction mixture was 4.10 and the reaction temperature was 140 ℃. Colorless flake-like crystals were obtained as a pure phase, confirmed by the powder XRD measurements (Fig.S1). Yield: 50.1% (based on 4-cnappH_3). Elemental analysis found (Calcd.) for $C_{11}H_9O_6PMn$(%): C, 40.66(40.89); H, 2.93(2.79). IR (KBr, cm^{-1}): 3 334 (b,m), 2 361(vs), 2 341(vs), 1 697(s), 1 618(m), 1 581 (w), 1 516(m), 1 459(w), 1 405(m), 1 285(m), 1 260(m), 1 205(w), 1 154(w), 1 124(m), 1 069(s), 1 025(s), 1 003 (s), 979(vs), 860(m), 794(w), 773(s), 679(s), 619(m).

1.3　Structure determination

Single crystals of dimensions 0.3 mm×0.1 mm×0.05 mm for **1**, 0.3 mm×0.02 mm×0.05 mm for **2**, 0.2 mm×0.15 mm×0.05 mm for **3**, and 0.3 mm×0.1 mm×0.1 mm for **4** were used for structural determination on a Bruker APEX DUO diffractometer (Mo $K\alpha$, λ=0.071 073 nm) at 123 K (for **1** and **2**) or Bruker APEX Ⅱ diffractometer (Mo $K\alpha$, λ=0.071 073 nm) at 296 K (for **3** and **4**). A total of 8 952, 18 518, 4 613 and 15 806 diffraction points were collected for compounds **1**~**4** in the range of $1.8° < \theta < 26.0°$, $2.1° < \theta < 26.0°$, $3.5° < \theta < 27.0°$ and $2.2° < \theta < 28.3°$, respectively, in which the independent diffraction points were 2 320 (**1**: R_{int}=0.046), 4 591 (**2**: R_{int}=0.057), 2 385 (**3**: R_{int}=0.032) and 2 761 (**4**: R_{int}=0.082), respectively. The observed diffraction points ($I>2.0\sigma(I)$) were 1 902, 3 788, 2 125 and 1 969 for **1**~**4**, respectively. The collected data were integrated by using the Siemens SAINT program[17], with the intensities corrected for the Lorentz factor, polarization, air absorption, and absorption due to variation in the path length through the detector face plate. Absorption corrections were applied. The structures were solved by direct methods and refined on F^2 by full-matrix least-squares by using SHELXTL[18]. All the non-hydrogen atoms were located from the Fourier maps and were refined anisotropically. The organic groups in **3** and **4** are disordered over two sites. The disordered atoms were refined anisotropically. All hydrogen atoms bound to carbon were refined isotropically in the riding mode; hydrogen atoms bound to phosphonate and carboxylate oxygen were calculated on idealized positions by taking into account C-O and P-O bond lengths; hydrogen atoms of water molecules were detected in the experimental electron density map and then refined isotropically with reasonable restriction of O-H bond distances and H-O-H angles. The crystallographic data of the compounds are listed in Table 1. Selected bond lengths and angles are given in Table 2.

CCDC: 1990441, **1**; 1990442, **2**; 1990443, 3; 1990444, **4**.

Table 1　Crystallographic data for compounds 1~4

Compound	1	2	3	4
Formula	$C_{22}H_{16}O_{10}P_2Mn$	$C_{22}H_{20}O_{12}P_2Mn$	$C_{11}H_9O_6PMn$	$C_{11}H_9O_6PMn$
Formula weight	557.23	593.26	323.09	323.09
Crystal system	Orthorhombic	Monoclinic	Triclinic	Monoclinic
Space group	*Pbcn*	$P2_1/c$	$P\bar{1}$	$P2_1/n$
a / nm	1.749 7(2)	1.994 2(1)	0.525 4(1)	0.513 4(1)

Continued Table 1

b / nm	1.458 0(1)	0.811 7(1)	0.600 2(1)	3.719 5(4)
c / nm	0.929 6(1)	1.520 1(1)	1.817 9(3)	0.588 9(1)
α / (°)			85.066(4)	
β / (°)		107.033(1)	88.329(5)	97.361(1)
γ / (°)			78.332(4)	
V / nm^3	2.371 6(4)	2.352 5(3)	0.559 4(2)	1.115 3(2)
Z	4	4	2	4
D_c / (g·cm^{-3})	1.561	1.675	1.918	1.924
μ / mm^{-1}	0.747	0.764	1.343	1.347
F(000)	1 132.0	1 212.0	326.0	652.0
GOF on F^2	1.001	0.999	0.990	1.007
R_1, wR_2[a] [$I>2\sigma(I)$]	0.036 7, 0.086 7	0.035 2, 0.085 0	0.075 8, 0.191 1	0.065 5, 0.128 5
R_1, wR_2 (all data)	0.048 0, 0.093 9	0.045 7, 0.911	0.084 0, 0.197 6	0.109 4, 0.156 1
$(\Delta\rho)_{max}$, $(\Delta\rho)_{min}$ / (e·nm^{-3})	382, −419	394, −432	1 427, −847	597, −642

[a] $R_1=\sum||F_o|-|F_c||/\sum|F_o|$, $wR_2=[\sum w(F_o^2-F_c^2)^2/\sum w(F_o^2)^2]^{1/2}$

Table 2 Selected bond lengths (nm) and bond angles (°) for compounds 1~4

			1		
Mn1-O2A	0.215 0(2)	Mn1-O1C	0.216 2(2)	Mn1-O4	0.220 0(2)
O2A-Mn1-O2B	92.0(1)	O2A-Mn1-O1C	96.2(1)	O2A-Mn1-O1D	92.7(1)
O2B-Mn1-O4	89.9(1)	O1C-Mn1-O4	84.7(1)	O1D-Mn1-O4	86.1(1)
O1C-Mn1-O1D	167.2(1)	O2A-Mn1-O4	177.8(1)	O4-Mn1-O4E	88.2(1)
			2		
Mn1-O1	0.222 0(2)	Mn1-O2A	0.215 9(2)	Mn1-O5B	0.218 5(2)
Mn1-O4	0.209 7(2)	Mn1-O1W	0.220 9(2)	Mn1-O2W	0.223 0(2)
O4-Mn1-O2A	93.7(1)	O4-Mn1-O5B	100.0(1)	O2A-Mn1-O5B	166.3(1)
O4-Mn1-O1W	94.1(1)	O2A-Mn1-O1W	94.4(1)	O5B-Mn1-O1W	84.5(1)
O4-Mn1-O1	173.8(1)	O2A-Mn1-O1	81.4(1)	O5B-Mn1-O1	85.0(1)
O1W-Mn1-O1	89.9(1)	O4-Mn1-O2W	85.9(1)	O2A-Mn1-O2W	94.6(1)
O5B-Mn1-O2W	86.6(1)	O1W-Mn1-O2W	171.0(1)	O1-Mn1-O2W	90.8(1)
			3		
Mn1-O1	0.208 4(6)	Mn1-O2B	0.214 3(5)	Mn1-O2C	0.218 2(5)
Mn1-O3A	0.206 6(6)	Mn1-O1W	0.220 4(6)		
O3A-Mn1-O1	129.0(3)	O3A-Mn1-O2B	114.9(3)	O1-Mn1-O2B	115.6(2)
O3A-Mn1-O2C	92.5(2)	O1-Mn1-O2C	91.1(2)	O2B-Mn1-O2C	77.9(2)
O3A-Mn1-O1W	92.6(3)	O1-Mn1-O1W	95.7(2)	O2B-Mn1-O1W	88.2(2)
O2C-Mn1-O1W	166.1(2)	Mn1-O2B-Mn1C	102.1(2)		
			4		
Mn1-O1	0.215 0(4)	Mn1-O1C	0.219 4(4)	Mn1-O2A	0.212 2(4)
Mn1-O3B	0.215 0(4)	Mn1-O1W	0.219 5(4)		
O2A-Mn1-O3B	91.4(1)	O2A-Mn1-O1	93.6(1)	O3B-Mn1-O1	105.8(1)

Continued Table 2

O2A-Mn1-O1C	89.7(1)	O3B-Mn1-O1C	109.5(1)	O1-Mn1-O1C	144.5(2)
O2A-Mn1-O1W	168.8(2)	O3B-Mn1-O1W	98.8(1)	O1-Mn1-O1W	88.1(1)
O1C-Mn1-O1W	82.6(1)	Mn1-O1C-Mn1C	116.1(2)		

Symmetry codes: A: 1/2+*x*, 1/2+*y*, 3/2−*z*; B: 3/2−*x*, 1/2+*y*, *z*; C: 3/2−*x*, 3/2−*y*, −1/2+*z*; D: 1/2+*x*, 3/2−*y*, 2−*z*; E: 2−*x*, *y*, 3/2−*z* for **1**; A: −*x*, −1/2+*y*, 1/2−*z*; B: −*x*, −*y*, 1−*z* for **2**; A: 1−*x*, 1−*y*, 2−*z*; B: *x*, 1+*y*, *z*; C: −*x*, 1−*y*, 2−*z* for **3**; A: 1/2+*x*, 1/2−*y*, −1/2+*z*; B: *x*, *y*, −1+*z*; C: −1/2+*x*, 1/2−*y*, −1/2+*z* for **4**.

2　Results and discussion

2.1　Crystal structures of 1 and 2

Compounds **1** and **2** were synthesized under similar solvothermal reaction conditions in water/methanol solution except the pH value of the reaction mixture (3.05 for **1**, and 3.80 for **2**, Scheme 1). Although the chemical composition of **2** is different from that of **1** by two additional water molecules, their structures are completely different.

Single crystal structural determination reveals that **1** crystalizes in orthorhombic system space group *Pbcn*. The asymmetric unit consists of 0.5 Mn atom and one 4-cnappH$_2^-$ ligand. The Mn atom has an octahedral geometry with the six sites occupied by four phosphonate oxygen and two carboxylate oxygen atoms from six equivalent 4-cnappH$_2^-$ ligands (Fig.1a and S4a, Table 2). The Mn-O bond lengths (0.215 0(2) ~0.220 0(2) nm) are comparable to those in the other manganese phosphonate compounds[19].

Each 4-cnappH$_2^-$ acts as a tri-dentate bridging ligand, binding to three equivalent Mn atoms via two phosphonate oxygen (O2, O3) and one carboxylate oxygen (O4) atoms (Scheme 2a). The remaining one phosphonate oxygen (O3) and one carboxylate oxygen (O5) atoms are protonated. As a result, the equivalent Mn atoms are doubly bridged by the O-P-O units forming infinite chains running along the c-axis with extensive intrachain hydrogen bond interactions (Fig. 1a). The neighboring chains are cross-linked by the organic groups of 4-cnappH$_2^-$, leading to a three-dimensional framework structure (Fig.1b). The shortest Mn⋯Mn distances are 0.528 4 nm within the chain and 1.138 8 nm between the chains.

Compound *2* crystallizes in monoclinic space group $P2_1/c$. The asymmetric unit contains one Mn, two 4-cnappH$_2^-$ and two water molecules. The Mn atom is again octahedrally coordinated but by four phosphonate oxygen atoms (O1, O2A, O4, O5B) and two water molecules (O1W, O2W) (Mn-O 0.209 7(1)~

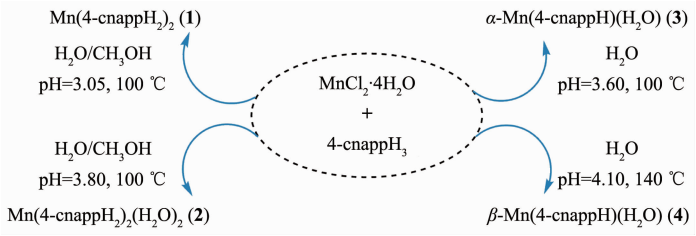

Scheme 1　Synthetic routes of compounds **1**~**4**

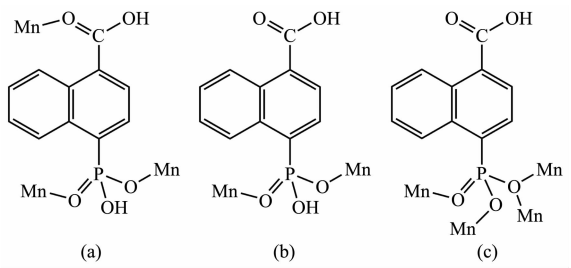

Scheme 2　Coordination modes of 4-cnappH$_3$ in compounds **1** (a), **2** (b), **3** and **4** (c)

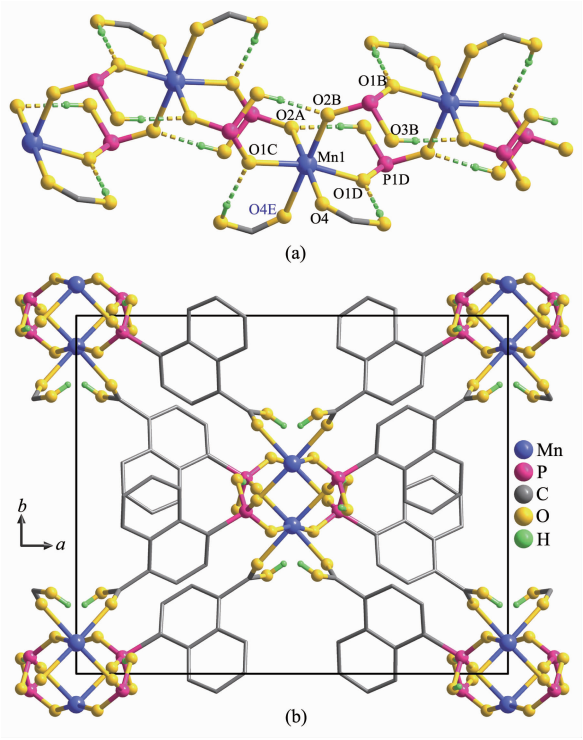

Symmetry codes: A: 1/2+x, 1/2+y, 3/2−z; B: 3/2−x, 1/2+y, z; C: 3/2−x, 3/2−y, −1/2+z; D: 1/2+x, 3/2−y, 2−z; E: 2−x, y, 3/2−z

Fig.1 (a) Single chain structure of compound **1**; (b) Packing diagram of structure **1**

0.223 0(1) nm, ∠O-Mn-O=84.5(1)°~173.8(1)°, Fig.2a and S4b, Table 2), unlike that in **1** where the carboxylate oxygen atoms occupy two sites. In addition, each 4-cnappH_2^- ligand binds to two instead of three equivalent Mn atoms using two of its three phosphonate oxygen donors, leaving both carboxylate oxygen atoms pendant (Scheme 2b). The {MnO_6} octahedra and {PO_3C} tetrahedra are corner-shared with each other alternatively, forming an inorganic layer containing rectangular-shaped 12-membered rings of Mn_6P_6 (Fig.2a). The Mn⋯Mn distances within the layer are 0.519 2 and 0.511 6 nm over O-P1-O and O-P2-O units, respectively. Extensive hydrogen bond interactions are present within the layer among the phosphonate oxygen atoms and coordination water molecules. The layers are stacked along the *a*-axis with the 4-carboxynaphthalen-1-yl groups filling in the interlayer space (Fig.2b). Hydrogen bond interactions are found between the protonated carboxylic groups of the adjacent layers (O7⋯O9A 0.266 8(135) nm, O10⋯O9A 0.269 5(127) nm, Symmetry code: A: 1+x, 1+y, z). The interlayer distance is 1.905 8 nm.

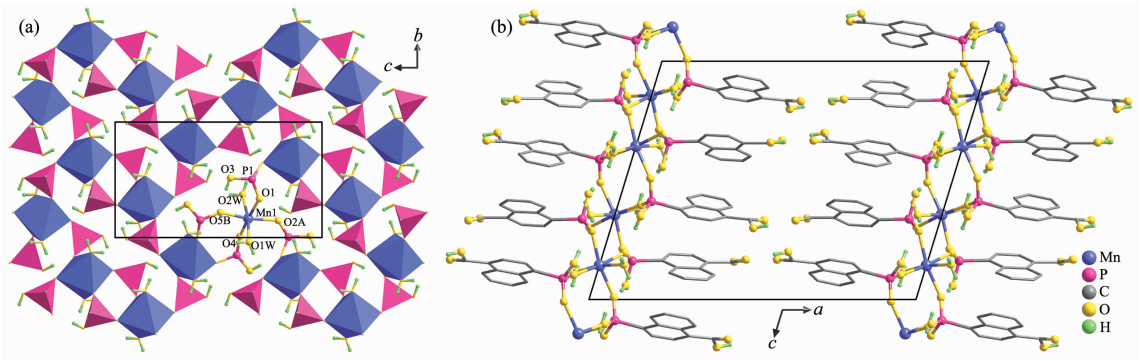

Symmetry codes: A: −x, −1/2+y, 1/2−z; B: −x, −y, 1−z

Fig.2 (a) Inorganic layer in structure **2**; (b) Packing diagram of structure **2**

2.2 Crystal structures of 3 and 4

Compounds **3** and **4** were synthesized under hydrothermal conditions at different temperatures (Scheme 1). They are isomers with the same molecular formula, but crystallize in different space groups, triclinic $P\bar{1}$ for **3** and monoclinic $P2_1/n$ for **4**. In both cases, the asymmetric unit is composed of one Mn, one 4-cnppH_2^- and one water molecule. The Mn atoms in **3** and **4** have distorted trigonal bipyramidal geometries (Fig.S5a and S5b), unlike those in **1** and **2**. For **3**, three equatorial sites of {MnO_5} are occupied by the phosphonate oxygen atoms (O1, O2B, O3A), and the axial positions by phosphonate oxygen atom (O2C) and one water (O1W) (Mn-O 0.206 3(6)~0.218 1(5) nm) (Fig.3a). The sum of equatorial O-Mn-O angles, ranging from 114.9° to 129.0°, is 359.5°. The axial O2C-Mn1-O1W angle is 166.1°. The {MnO_5} geometry in **4** is more distorted with the equatorial O-Mn-O

angles ranging from 105.8° to 144.5° and the axial O-Mn-O angle of 168.8° (Fig.3c). The coordination modes of the 4-cnppH_2^- ligands are also quite similar in **3** and **4**, each serves as a tetra-dentate ligand connecting four Mn atoms using its three phosphonate oxygen donors, one of which serves as a μ_3-O bridge (Scheme 2c). The carboxylate groups are protonated and not involved in coordination with metal ions. Remarkably, although both show layer structures, their layer topologies are significantly different. In **3**, two equivalent $\{MnO_5\}$ are edge-shared with each other forming $\{Mn_2O_2\}$ dimers (∠Mn1-O2B-Mn1C=102.1(2)°). The dimers are further connected by O-P-O linkages, forming an inorganic layer containing 4-membered rings of Mn_2P_2 (Fig.3a). In **4**, the equivalent $\{MnO_5\}$ are corner-shared with each other forming chains of Mn-O-Mn-O (∠Mn1-O1C-Mn1C=116.1(2)°), which are connected by the $\{PO_3C\}$ tetrahedra via corner-sharing of $\{MnO_5\}$ and $\{PO_3C\}$ into an inorganic layer containing 3- and 4-membered rings of Mn_2P and Mn_2P_2 (Fig.3c). The different topologies result in different Mn⋯Mn distances within the layer. The Mn⋯Mn distances over the μ_3-O bridge in **3** (0.336 4 nm) is shorter than that in **4** (0.368 6 nm). Those over the O-P-O bridges are 0.391 7, 0.414 6 and 0.471 4 nm in **3**, and 0.417 8 and 0.513 4 nm in **4**. The layers are stacked along the *c*-axis (for 3) or *b*-axis (for **4**) with interlayer hydrogen bond interactions through the carboxylic acid groups, thus leading to 3D supramolecular frameworks (Fig.3b and 3d).

It is worth mentioning that there are only four compounds reported so far based on the same phosphonate ligand. Compound Co_2(4-cnapp)(OH)$(H_2O)_2$ has a 3D framework structure in which the Δ-type chains of corner-sharing $Co_3(\mu_3$-OH) triangles are cross-linked by the organic groups of the phosphonate ligands. Compounds α-Cu(4-cnappH)(H_2O) and α-Cu(4-cnappH)$(H_2O)\cdot 0.5H_2O$ display layer structures containing 4- and 8-membered rings made up of $\{CuO_4\}$ planes and $\{PO_3C\}$ tetrahedra. In β-Cu(4-cnappH)(H_2O), the layer topology is composed of edge-sharing dimers of $\{CuO_5\}$ square pyramids and $\{PO_3C\}$ linkages which is similar to that in **3**. Therefore, compounds **1**, **2** and **4** provide new types of structures of metal

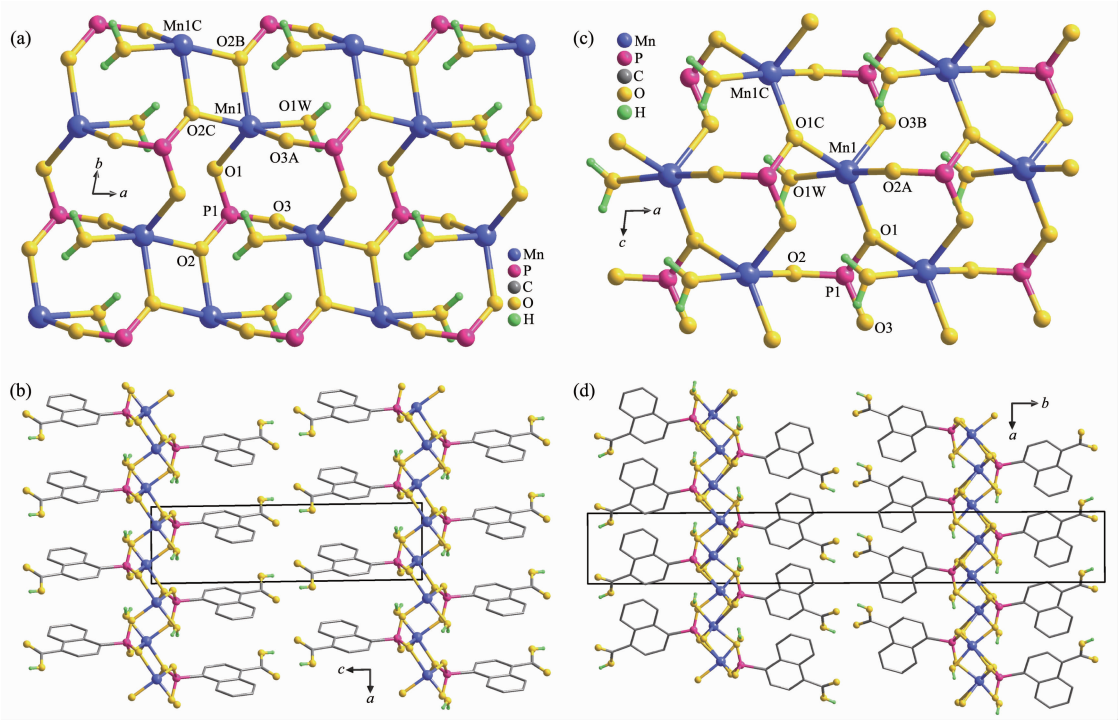

Only one part of the disordered moieties are shown in (b); Only one part of the disordered moieties are shown in (d); Symmetry codes: A: 1−*x*, 1−*y*, 2−*z*; B: *x*, 1+*y*, *z*; C: −*x*, 1−*y*, 2−*z* for **3**; A: 1/2+*x*, 1/2−*y*, −1/2+*z*; B: *x*, *y*, −1+*z*; C: −1/2+*x*, 1/2−*y*, −1/2+*z* for **4**

Fig.3　(a) Inorganic layer and (b) packing diagram of structure 3; (c) Inorganic layer and (d) packing diagram of structure **4**

phosphonates based on (4-carboxynaphthalen-1-yl) phosphonate ligand. As far as we are aware, the layer topology of **4** has not been observed in the other layered metal phosphonate materials.

2.3 Magnetic properties

Temperature dependent magnetic susceptibilities were measured for **1**~**4** in a temperature range of 1.8~300 K. The observed room temperature $\chi_M T$ values per Mn unit were 4.43 $cm^3 \cdot K \cdot mol^{-1}$ for **1**, 5.00 $cm^3 \cdot K \cdot mol^{-1}$ for **2**, 4.40 $cm^3 \cdot K \cdot mol^{-1}$ for **3**, and 4.26 $cm^3 \cdot K \cdot mol^{-1}$ for **4**, which are close to the theoretical value (4.38 $cm^3 \cdot K \cdot mol^{-1}$) for one Mn(Ⅱ) ion with g=2.0. Upon cooling, the $\chi_M T$ values decreased with decreasing temperature in all cases, indicating that dominant antiferromagnetic (AF) interactions are propagated between the Mn(Ⅱ) ions.

For **1**, there exists O-P-O bridged equally spaced manganese chains, inter-connected by the organic groups. The Mn ⋯ Mn distances within the chain (0.528 4 nm) is much shorter than that between the chains (1.138 8 nm). Thus the magnetic susceptibility data can be analyzed using Fisher′s expression for a uniform chain based on Hamiltonian $\boldsymbol{H}=-J\sum \boldsymbol{S}_A\boldsymbol{S}_{A+1}$, with the classical spins scaled to a real quantum spin of S=5/2[16], leading to parameters g=2.03, J=−0.13 cm^{-1} (Fig.4). The negative exchange coupling constant (J) confirms the presence of weak AF interactions. This value is close to those in $[NH_3(CH_2)_4NH_3][Mn(hedpH_2)_2]$ (J=−0.18 cm^{-1})[20] and $Mn\{(C_7H_5N_2)CH_2N(CH_2PO_3H)_2\}$ (J=−0.08 cm^{-1})[21] which also contain manganese chains with O-P-O linkages.

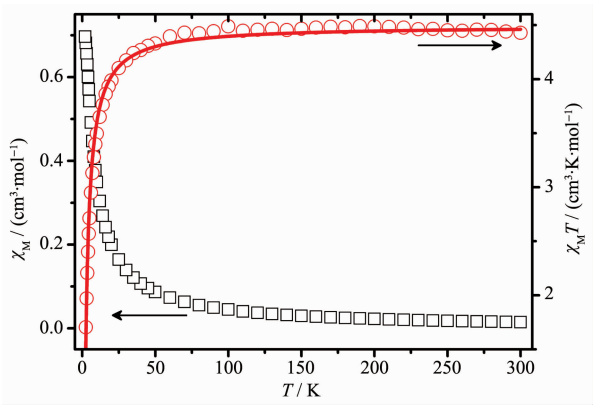

Solid line is the best fit to a chain model

Fig.4 χ_M vs T (black) and $\chi_M T$ vs T (red) plots for **1**

Compound **2** has a layer structure containing rectangular-shaped 12-membered rings in which each Mn is linked to three equivalents via O-P-O units. The Mn⋯Mn distances within the layer are 0.519 2 and 0.511 6 nm. It is difficult to find a suitable model to fit the susceptibility data. Hence the data were simply fitted by the Curie-Weiss law, leading to the Curie constant of 4.29 $cm^3 \cdot K \cdot mol^{-1}$ and Weiss constant (θ) of −1.56 K (Fig.S7). The negative θ value also confirms the presence of AF interactions in **2**.

For **3**, the layer structure is composed of $\{Mn_2O_2\}$ dimers inter-connected by O-P-O units. Assuming that the exchange coupling within the dimer over μ_3-O(P) bridge (J) is much stronger than that over the O-P-O bridge between the dimers (zJ'), the susceptibility data can be analyzed by an isotropic dimer model for two S=5/2 spins based on the Heisenberg Hamiltonian $\boldsymbol{H}=-J\boldsymbol{S}_A\boldsymbol{S}_B$ [16]. The best fit gave parameters g=2.03, J=−0.82 cm^{-1}, zJ'=0 (fixed) (Fig.5). The exchange coupling constant is more negative than that for **1**, in agreement with the stronger AF interaction mediated over the μ_3-O(P) bridge than that over the O-P-O linkage. The J value also agrees well with those for the other manganese phosphonates containing μ_3-O(P) bridged $\{Mn_2O_2\}$ dimers[20]. The magnetization measured at 2.0 K showed a slight sigmoid curve (Fig.5, Inset). The M value increased linearly with increasing field from zero to 18.8 kOe, above which it increased faster. The result is indicative of a spin flipping behavior from AF group state of the material.

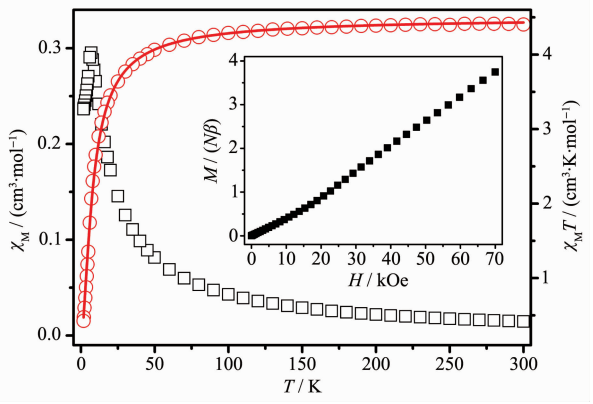

Solid line is the best fit to a dimer model; Inset: Magnetization curve of **3** at 2.0 K

Fig.5 χ_M vs T (black) and $\chi_M T$ vs T (red) plots for **3**

In the case of **4**, chains of Mn-O-Mn-O are separated by the O-P-O units within the inorganic layer. Both the negative Weiss constant (−36.1 K) and the maximum appearing at 7.5 K in the χ_M vs T curve support the presence of AF interactions between the magnetic centers (Fig.S8a). However, an attempt to fit the susceptibility data using Fisher′s chain model could not give a reasonable result, indicating that the exchange couplings propagated through μ_3-O(P) and O-P-O bridges are comparable. The magnetization curve again reveals a spin flipping behavior with the critical field of 20 kOe at 2.0 K (Fig.S8b).

3 Conclusions

We report four manganese phosphonates based on (4-carboxynaphthalen-1-yl)phosphonic acid, namely, Mn(4-cnappH$_2$)$_2$ (**1**), Mn(4-cnappH$_2$)$_2$(H$_2$O)$_2$ (**2**), α-Mn(4-cnappH)(H$_2$O) (**3**) and β-Mn(4-cnappH)(H$_2$O) (**4**), simply by modifying the reaction conditions such as the solvent and the pH of the reaction mixture. Compound **1** shows a 3D framework structure containing inorganic chains, whereas **2**~**4** exhibit 2D layered structures with different topologies of the inorganic layers. Antiferromagnetic interactions are found to be dominant in all four compounds. Spin flipping behavior is observed in compounds **3** and **4**.

Supporting information is available at http://www.wjhxxb.cn

References:

[1] (a)Kirchon A, Feng L, Drake H F, et al. *Chem. Soc. Rev.*, **2018**,**47**:8611-8638
(b)Dhaka S, Kumar R, Deep A, et al. *Coord. Chem. Rev.*, **2019**,**380**:330-352
(c)Wang H, Lustig WP, Li J. *Chem. Soc. Rev.*, **2018**,**47**:4729-4756

[2] (a)Wang Q, Astruc D. *Chem. Rev.*, **2020**,**120**:1438-1511
(b)Dhakshinamoorthy A, Li Z H, Garcia H. *Chem. Soc. Rev.*, **2018**,**47**:8134-8172
(c)Wang H F, Chen L, Pang H, et al. *Chem. Soc. Rev.*, **2020**, **49**:1414-1448

[3] (a)Cui Y, Zhang J, He H, et al. *Chem. Soc. Rev.*, **2018**,**47**:5740-5785
(b)Jia J G, Zheng L M. *Coord. Chem. Rev.*, **2020**,**403**:213083
(c)Thorarinsdottir A E, Harris T D. *Chem. Rev.*, **2020**,doi:10.1021/acs.chemrev.9b00666.

[4] (a)Clearfield A. *Progress in Inorganic Chemistry*: *Vol.*47. New York: John Wiley & Sons, **1998**:371-510
(b)Clearfield A, Demadis K. Ed. *Metal Phosphonate Chemistry*: *From Synthesis to Applications*. Cambridge: RSC Publishing, **2012**.

[5] Mao J G. *Coord. Chem. Rev.*, **2007**,**251**:1493-1520

[6] Shearan S J, Stock N, Emmerling F, et al. *Crystals*, **2019**,**9**:270

[7] Bhanja P, Na J, Jing T, et al. *Chem. Mater.*, **2019**,**31**:5343-5362

[8] (a)Bao S S, Zheng L M. *Coord. Chem. Rev.*, **2016**,**319**:63-85
(b)Bao S S, Shimizu G K H, Zheng L M. *Coord. Chem. Rev.*, **2019**,**378**:577-594
(c)Weng G G, Zheng L M. *Sci. China Chem.*, **2020**,doi:10.1007/s11426-020-9707-4

[9] (a)Zima V, Svoboda J, Benes L, et al. *J. Solid State Chem.*, **2009**,**182**:3155-3161
(b)Zang D M, Cao D K, Zheng L M. *Inorg. Chem. Commun.*, **2011**,**14**:1920-1923
(c)Wang P F, Duan Y, Cao D K, et al. *Dalton Trans.*, **2010**, **39**:4559-4565
(d)Adelani P O, Albrecht-Schmitt T E. *Inorg. Chem.*, **2010**, **49**:5701-5705
(e)Adelani P O, Albrecht-Schmitt T E. *Cryst. Growth Des.*, **2011**,**11**:4676-4683
(f)Chen Z X, Yang H Y, Deng M L, et al. *Dalton Trans.*, **2012**,**41**:4079-4083
(g)Deng M L, Liu X F, Zheng Q S, et al. *CrystEngComm*, **2013**,**15**:7056-7061
(h)Dai L L, Zhu Y Y, Jiao C Q, et al. *CrystEngComm*, **2014**, **16**:5050-5061
(i)Rueff J M, Perez O, Caignaert V, et al. *Inorg. Chem.*, **2015**,**54**:21522159

[10](a)Li J T, Keene T D, Cao D K, et al. *CrystEngComm*, **2009**, **11**:1255-1260
(b)Wang P F, Cao D K, Bao S S, et al. *Dalton Trans.*, **2011**, **40**:1307-1312
(c)Putz A M, Carrella L M, Rentschler E. *Dalton Trans.*, **2013**,**42**:16194-16199

[11](a)Li J T, Cao D K, Akutagawa T, et al. *Dalton Trans.*, **2010**, **39**:8606-8608
(b)Wang P F, Bao S S, Huang X D, et al. *Chem. Commun.*, **2018**,**54**:6276-6279

[12]Yang X J, Bao S S, Zheng T, et al. *Chem. Commun.*, **2012**, **48**:6565-6567

[13]Liu B, Xu Y, Bao S S, et al. *Inorg. Chem.*, **2016**,**55**:95219523

[14]Liu B, Liu J C, Shen Y, et al. *Dalton Trans.*, **2019**,**48**:6539-6545

[15]Zheng T, Bao S S, Ren M, et al. *Dalton Trans.*, **2013**,**42**:16396-16402

[16]Kahn O. *Molecular Magnetism*. New York: VCH Publishers, Inc., **1993**.

[17]*SAINT, Program for Data Extraction and Reduction*, Siemens Analytical X-ray Instruments, Madison, WI, **1994-1996**.

[18]*SHELXTL, Ver*.5.0, *Reference Manual*, Siemens Industrial Automation, Analytical Instruments, Madison, WI, **1995**.

[19](a)Jin H J, Wang P F, Bao S S, et al. *Sci. China Chem.*, **2012**,**55**:1047-1054

(b)YANG Xiao-Jing (杨骁婧), BAO Song-Song(鲍松松), ZHENG Li-Min(郑丽敏). *Chinese J. Inorg. Chem.*(无机化学学报), **2013**,**29**:621-627

[20]Song H H, Yin P, Zheng L M, et al. *J. Chem. Soc. Dalton Trans.*, **2002**:2752-2759

[21]Cao D K, Xiao J, Li Y Z, et al. *Eur. J. Inorg. Chem.*, **2006**:1830-1837